8.3 A Comparison of Two Coastal Barrier Jets along the Southeast Alaskan Coast during the SARJET Field Experiment

Joseph Olson[1], Brian A. Colle[1*], Nicholas A. Bond[2], and Nathaniel Winstead[3]

[1]Institute for Terrestrial and Planetary Atmospheres, Stony Brook University/SUNY
[2]Joint Institute for the Study of Atmosphere and Ocean, University of Washington
[3]Johns Hopkins University, Applied Physics Laboratory

1. Introduction

Strong low-level terrain-parallel winds, known as barrier jets (Parish 1982), can reach high speeds (> 30 m s^{-1}) and are commonly observed along coastal southeastern Alaska (Loesher et al. 2005; Overland and Bond 1993 and 1995; Macklin et al. 1990). During the cool season, this region frequently experiences a large-scale flow configuration that favors the development of barrier jets, such as an anomalously deep upper-level trough over the Aleutian Islands and an anomalous ridge aloft over western Canada (Colle et al. 2006). This configuration produces a mean low-level southerly flow that impinges on the large and steep coastal terrain, producing many hazardous barrier jet events that affect the local fishing, shipping, and aviation industries (Macklin et al. 1990).

Strong terrain-parallel winds generated by the above mechanisms are regarded as "classical" barrier jets (Loescher et al. 2006), since they assume a quasi-two dimensional terrain with flow impinging towards the barrier. Loesher et al. (2006) also discussed a "hybrid" barrier jet, which involved a nearby offshore-directed gap flow merging with a barrier jet near the coast. Colle et al. (2006) showed that these hybrid jets are favored when there is a cold air source over interior Alaska, which favors an offshore-directed pressure gradient. These offshore-directed gap flows are quite common, such as through the Fraser River gap (Mass et al. 1995); the Shelikof Straight (Lackmann and Overland 1989); Cook Inlet (Macklin et al. 1990); and the Strait of Juan de Fuca (Colle and Mass 2000; Doyle and Bond 2001).

The Southeastern Alaskan Regional Jets (SARJET) experiment was completed between 24 September and 21 October 2004 near Juneau, Alaska, with its objective to collect in situ aircraft observations of coastal jets (Fig. 1; Winstead et al. 2006). The SARJET study region represents a portion of the coast that is concave in shape and has a steep cluster of mountains known as the "Fairweathers", which rise over 3000 m within 50 km from the coast. The terrain in this region is also highly complex, with numerous coastal gaps. The Cross Island Sound, located to the immediate southeast of the Fairweathers, is a sea-level gap approximately 50 km wide, which allows for gap outflows as observed by a climatology performed by Loescher et al. (2006) and Synthetic Apeture Radar (SAR) observations (Winstead et al. 2006).

The goal of this study is to provide a detailed three-dimensional analysis of a classical barrier jet on 26 September 2004 (IOP1) and a hybrid barrier jet on 12 October 2004 (IOP7) and to obtain a better understand the flow and dynamical differences between the "classical" barrier jets versus hybrid jets.

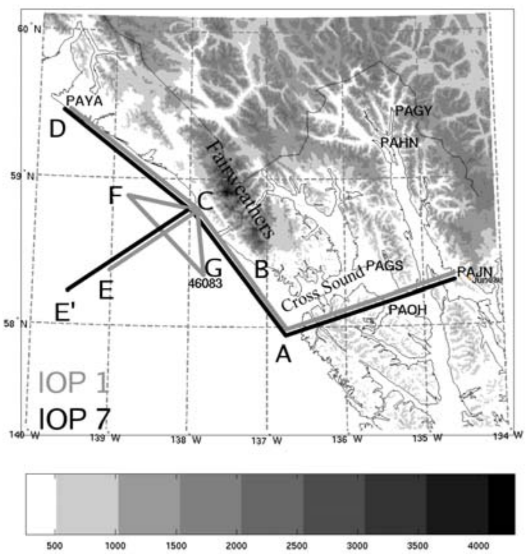

Figure 1. SARJET study region with flight tracks (IOP 1 gray; IOP 7 black) and terrain (gray shade).

2. Data and methods

Flight-level measurements for SARJET were obtained from the University of Wyoming's King Air research aircraft. Flight observations were collected from south of Cross Sound (pt. A in Fig. 1) to near Yakutat (pt. D), and from a series of four west-east flight legs at various altitudes from the coast (pt. C) to 75 – 120 km offshore (pts. E,E').

The Penn-State-NCAR Mesoscale Model (MM5; Grell et al. 1995) was used to further elucidate the dynamical and physical mechanisms for the SARJET cases. Three computational domains were used (Fig. 2b), with resolutions of 36-, 12-, and 4-kms. A 1.33-km nest was also run; however, the simulated structures were not significantly different than the 4-km nest along the coast, so the 1.33-km results are not highlighted in this paper. Thirty-two model sigma levels were used, with 14 levels below 700-hPa

The control model configuration for IOP 1 applied the Blackadar planetary boundary layer (PBL; Zhang and

Anthes 1982) scheme, while the 1.5-level closure (TKE-based) Mellor-Yamada (Mellor and Yamada 1974) was utilized for IOP7. For both IOPs, the Grell cumulus parameterization (Grell et al. 1995) was used on the 36- and 12- km domains, but the precipitation was explicitly resolved using the simple ice microphysical scheme (Dudhia 1989) in the 4-km domain.

The initial and boundary conditions were provided by the NCEP Global Forecast System (GFS) analyses at 1-deg resolution every 6 hours. Four-dimensional data assimilation (FDDA), as described in Stauffer and Seaman (1990), was applied to the 36-km domain in which moisture, temperature, and winds fields were nudged during the first 12-hours.

3. IOP 1: 26 September 2004

a. Synoptic evolution

The large-scale flow during the start of IOP1 at 1800 UTC 26 September 2004 is similar to the "classic" jet composite (Colle et al. 2006), with high amplitude 500-mb ridge over western North American and broad trough over western Alaska (not shown). Meanwhile, a surface cyclone over the northern Gulf of Alaska (see Winstead et al. Fig. 5) was well forecast by the 36-km MM5 at this time (Fig. 2a) as model sea-level pressure errors were typically < 1mb. Both the observations and model indicate a weak trough, which was preceded by enhanced low-level winds, extending south-southwest from the northernmost point of the Gulf of Alaska. The surface winds over the SARJET region were south-southeasterly at ~20-25 m s^{-1}.

b. Aircraft observations and model simulations

Aircraft dropsondes were not available upstream of the coast; however, the aircraft descended from 1000 to 300 m ASL about 90 km upstream of the coast (point E in Fig. 1) (not shown). The mean wind speed in this layer was ~28 m s^{-1} from south-southeast, which resulted in a cross-barrier wind component of ~8 m s^{-1}. Both model and observations also had a moist Brunt-Väisälä frequency of N_m~0.006 s^{-1}. This yielded a moist Froude number of ~0.8, thus the flow was in the partially blocked regime, with a Rossby radius of deformation ($N_m h/f$) of ~120 km

The observed winds veered 20-30^o to more coast-parallel between offshore point E and the coast (point C) (Fig. 3a). The winds increased from ~20 m s^{-1} offshore at point E to ~25 m s^{-1} at point C. The weak trough that moved into the study region during this period was likely responsible for much of this windshift, as suggested by the 4-km MM5 at 2200 UTC 26 September. The 4-km MM5 realistically simulated the veering winds at 150 m (Fig. 3b), but the model misplaced the maximum winds offshore by about 20-30 km. The observed and model winds show that the barrier jet maximum was located adjacent to and slightly downstream of the highest peak of the Fairweathers. At the 1000-m (Fig. 3c), a 40^o veering of the wind was observed between the ambient flows 80 km offshore and the coast, with a small wind speed enhancement from ~27 m s^{-1} at point E to ~30 m s^{-1} at the coast, which was well simulated by the model (Fig. 3d).

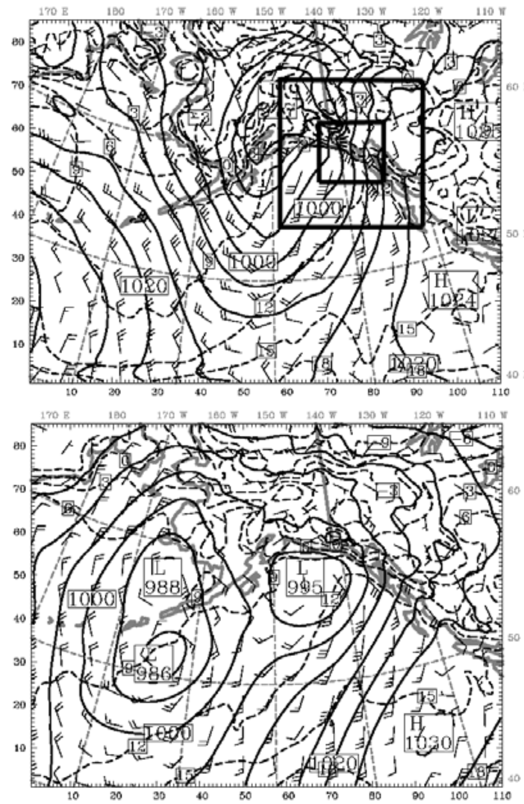

Figure 2. 36-km MM5 showing SLP (black every 5 mb), temperature (dashed every 3 ^{o}C), and winds barbs (full barb = 5 m s^{-1}) at (a) 1800 UTC 26 September 2004 and (b) 0000 UTC 13 October 2004.

A west to east cross-section of observed winds and potential temperatures was constructed using west to east flight legs at 1000, 300, 500, and 150 m between points C and E (Fig. 4). For flight 2 (2100 to 2350 UTC), the observed and simulated (valid for 22 UTC) wind speed component parallel to the coast increased from approximately 20 m s^{-1} offshore (point E) to over 30 m s^{-1} at the coast in the 500-1000-m layer. Above 2000 m ASL, the flow was considerably less blocked with winds speeds decreasing to <20 m s^{-1} and becoming nearly terrain-normal within 30 km from the coast.

4. IOP 7: 12-13 October 2004

a. Synoptic setting

At 0000 UTC 13 October 2004, there was an occluded (982 mb) surface low pressure near the Aleutian Islands in the 36-km MM5 (Fig. 2b), with a secondary weak cyclone (995 mb) located to the southeast, which was moving towards the SARJET study area, and there was a surface warm front to its southeast that was ~200 km offshore (west) of the coast. Both the observations and model had 5-10 ^{o}C colder inland surface temperatures for this IOP relative to IOP 1 (cf. Fig. 2a). For IOP7, there was a 1028 mb surface high over western Canada, which resulted in an offshore-directed pressure gradient and easterly flow through Cross Island Sound. The offshore warm front was about 3 hours too fast in the model, as

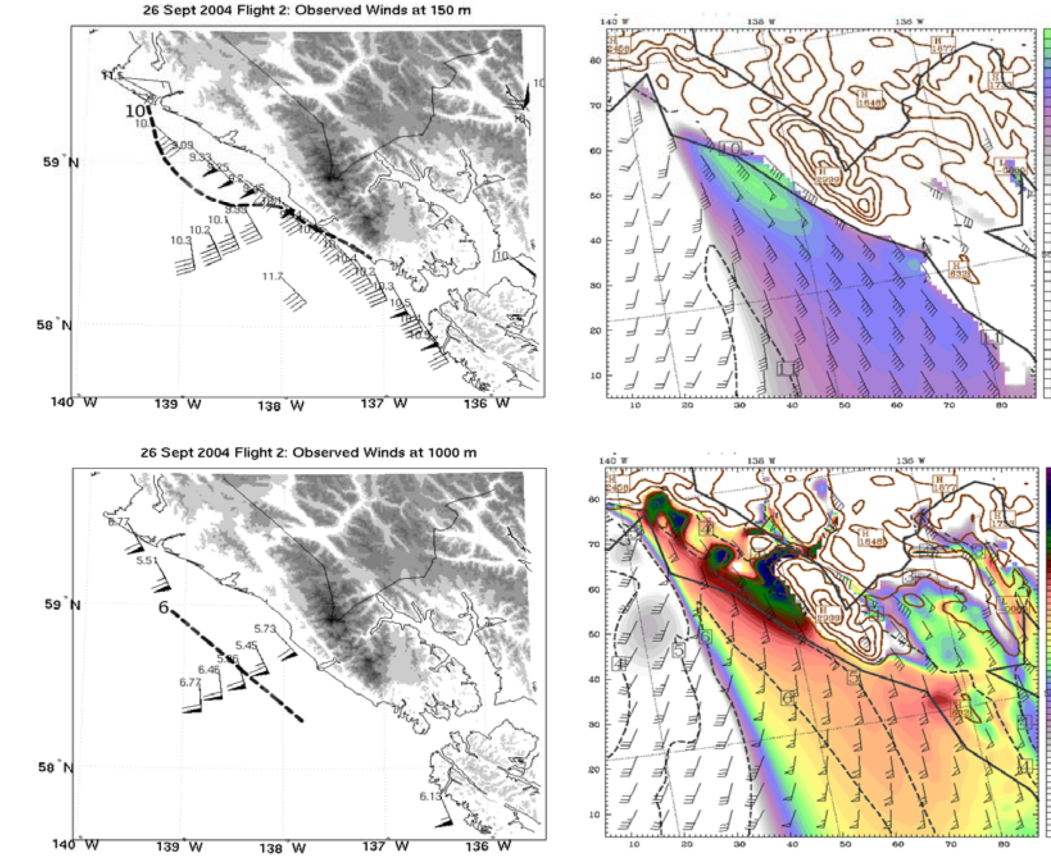

Figure 3. Winds (full barb = 5 m s^{-1}) and temperatures (dashed every 1 °C) at 150 m ASL for the (a) observations and (b) 4-km MM5 at 2100 UTC 26 September 2004. The model winds also shaded (in m s^{-1}) and terrain is contoured. (c) and (d) Same as (a) and (b) except at 1000 m

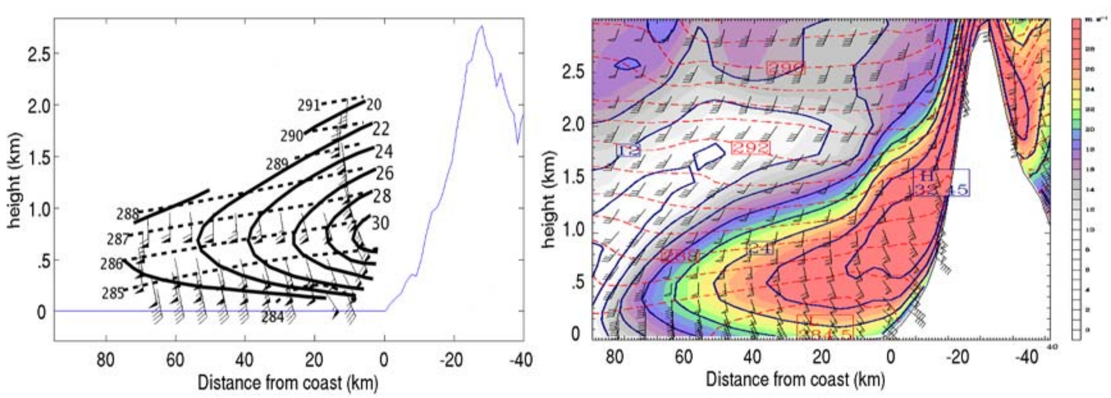

Figure 4. Vertical cross-section of winds (full barb = 5 m s^{-1}), terrain-parallel winds (solid every 4 m s^{-1}), and potential temperatures (dashed every 1 °C) between C-E for the (a) observations and (b) 4-km MM5 at 2100 UTC 26 September 2004. The model terrain-parallel winds are also shaded (in m s^{-1}).

revealed by the aircraft time series and frontal passage buoy 46083 (not shown). Therefore, in order to compare the model structures with the flight-level directly, the model analysis for time of flight 2 was shifted 3 hours, so the model simulation time used for flight 2 is 0200 – 0300 UTC rather than 2300 – 0000 UTC.

b. Aircraft observations and model simulations.

The King-Air aircraft ascended from 300 to 1000 m ASL about 130 km offshore at 0110 UTC (point E' in Fig. 1), which yielded a Froude number of 1.0 (N_m ~0.006 s^{-1}, U ~ 15 m s^{-1}) The 150-m level observed and 4-km MM5 winds (valid at 0200 UTC 13 Oct 2004) were southeasterly and exceeded 25 m s^{-1} 20-60 km

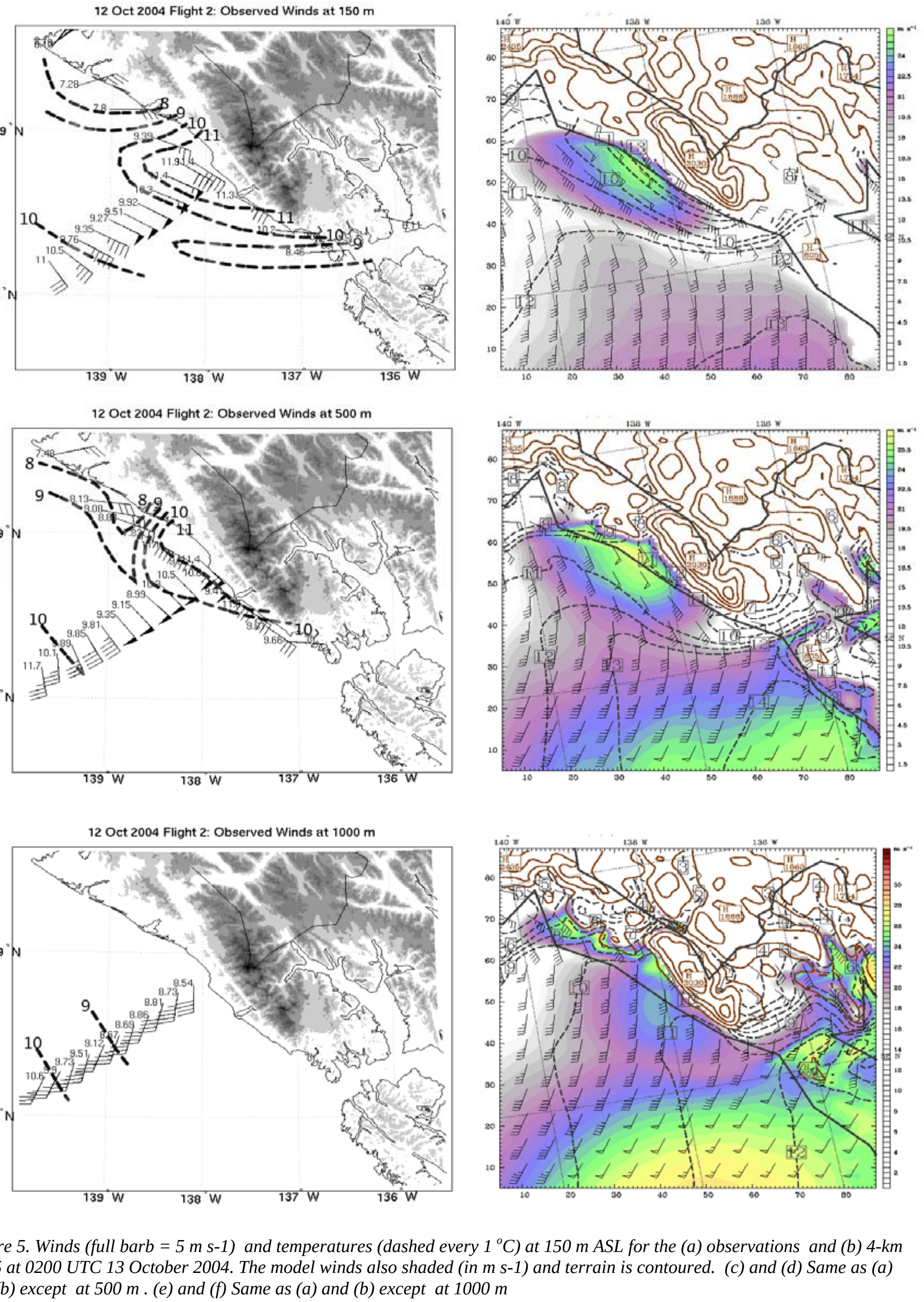

Figure 5. Winds (full barb = 5 m s-1) and temperatures (dashed every 1 °C) at 150 m ASL for the (a) observations and (b) 4-km MM5 at 0200 UTC 13 October 2004. The model winds also shaded (in m s-1) and terrain is contoured. (c) and (d) Same as (a) and (b) except at 500 m . (e) and (f) Same as (a) and (b) except at 1000 m

offshore of the coast (Figs. 5a,b). The low-level temperatures near the coast exceeded 11 ^{o}C, where there was a 5-10 m s^{-1} decrease in wind speeds. Meanwhile, the flow was more south-southeasterly at 15 m s^{-1} ~140 km offshore at point E', where the surface warm front was located. The surface temperature gradient was largest in the middle of the offshore flight leg, as the warm front interacted with the gap outflow from the Cross Sound. At 500 m ASL (Figs. 5c,d), there was a well-defined flow maximum exceeding 25 m s^{-1} about 80

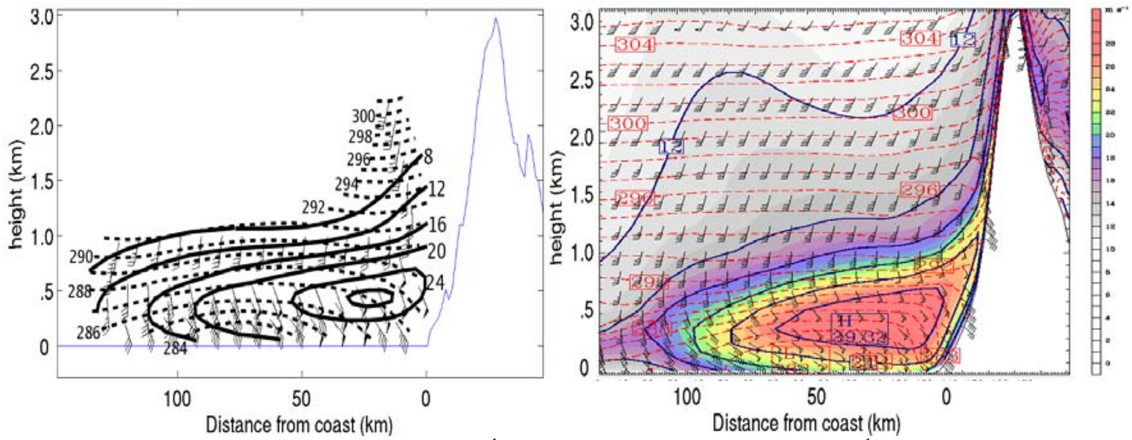

Figure 6. Vertical cross-section of winds (full barb = 5 m s^{-1}), terrain-parallel winds (solid every 4 m s^{-1}), and potential temperatures (dashed every 1 ^{o}C) between C-E at 0200 UTC 13 October 2004 for the (a) observations and (b) 4-km MM5 at 0200 UTC 13 October 2004. The model winds also shaded (in m s^{-1}) and terrain is contoured.

km upstream of the coast, while the winds were only ~13 m s^{-1} further offshore to the southwest of the warm front (point E'). The coldest temperatures associated with the cold gap outflow was ~30 km closer to the Fairweathers than at 150-m ASL, while a narrow (< 20 km) warm anomaly (+2 ^{o}C) persisted against windward slope of the barrier at 500 m ASL.

At 1000 m ASL (Figs. 5e,f), the south-southwesterly flow at 17 m s^{-1} accelerated to 20 m s^{-1} and become southerly at the coast. The simulated winds (Fig. 5f) were ~2-5 m s^{-1} too strong, but it accurately simulated the turning of winds upstream of the barrier. In contrast to the warm anomaly near the coast at 500 m, there was a ~1 ^{o}C cold anomaly near the coast at 1000-m. The deflection of the onshore flow to become more terrain-parallel, together with the cold anomaly found at this level, is more reminiscent of a "classical" barrier jet structure and what was observed in IOP1.

Figure 6 shows cross-sections of observed and simulated winds and potential temperatures for both flights. The observed winds show a well-defined barrier jet to 30 m s^{-1} within 100 km of the coast at 300-500 m ASL. The mean moist static stability (N_m~ 0.008 s^{-1} between 0 and 1000 m ASL) had increased slightly throughout the event as warm advection occurred over the gap outflow. The barrier jet was much weaker above 1-km ASL, with the winds more southerly at the 1000-m ASL and south-southwesterly at 2000-m ASL.

5. Trajectories and sensitivity tests

a. Trajectories

The three-dimensional structures presented for both IOPs suggest that there were different mechanisms responsible for the enhancement of the coastal winds. A central difference was the relatively cool gap outflow from the Cross Sound and warm air at the coast near the Fairweathers during IOP7. To help illustrate the origin of these coastal wind and temperature structures, backwards trajectories were calculated along cross-section C-E sampled by the research aircraft for both IOPs. A time step of 10 minutes was used with the spatial and temporal interpolation of hourly model data. The times of release were 2300 UTC and 0100 UTC for IOP 1 and IOP 7, respectively.

Figure 7 shows the trajectories released during each IOP for the 150- and 500-m level. The relatively uniform south-southeasterly winds of IOP 1 are evident in all the near-coast trajectories (3-6 in Fig. 7a and 9-12 in Fig. 7b), while all trajectories originate offshore at both the 150- and 500-m levels. The parcels released at the coast (#6 and #12) show a slight deflection to more east-southeasterly near the Fairweathers. The trajectories flow at both levels are confluent at about 120 km west of the coast, with a greater onshore components for trajectories 1-2 and 7-8 are evident, due to the windshift observed at the weak trough offshore immediately west of the strongest winds.

IOP 7 trajectories 3 and 4 at the 150-m level, released in or near the jet maximum within 100 km of the coast, all originate inland (Fig. 7c). Trajectories 5 and 6 are not part of the gap outflow from the Cross Sound, rather they follow the coastline, ascending the gap outflow to 1900 m and then descend adjacent to the Fairweathers to create the warm anomaly seen in Fig. 5. The trajectories released at the 500-m level (Fig. 7d) resemble more that of IOP 1 trajectories at this level (cf. Fig. 7b), with offshore origins and confluent flow 100-150 km from the coast. The two innermost trajectories (#11 and 12) descend from ~1300 m over the gap outflow to 500 m at the base of the Fairweathers. The trajectories furthest offshore at this level originate over the Pacific Ocean and are predominantly southerly.

b. Impact of local gap outflow

One of the questions this study attempts to address is how the gap outflow influenced the structure and intensity of the barrier jet during IOP 7. To examine the influence, the gap was removed (similar to Doyle and Bond, 2001) in order to seal the outflow from the Cross Sound. The simulation was then rerun to develop a barrier jet with the same synoptic forcing, but without the mesoscale gap outflow (NOGAP experiment). Figures 8a and b shows a snap-shot of the winds and temperature at the 150-m level for the CTL and NOGAP

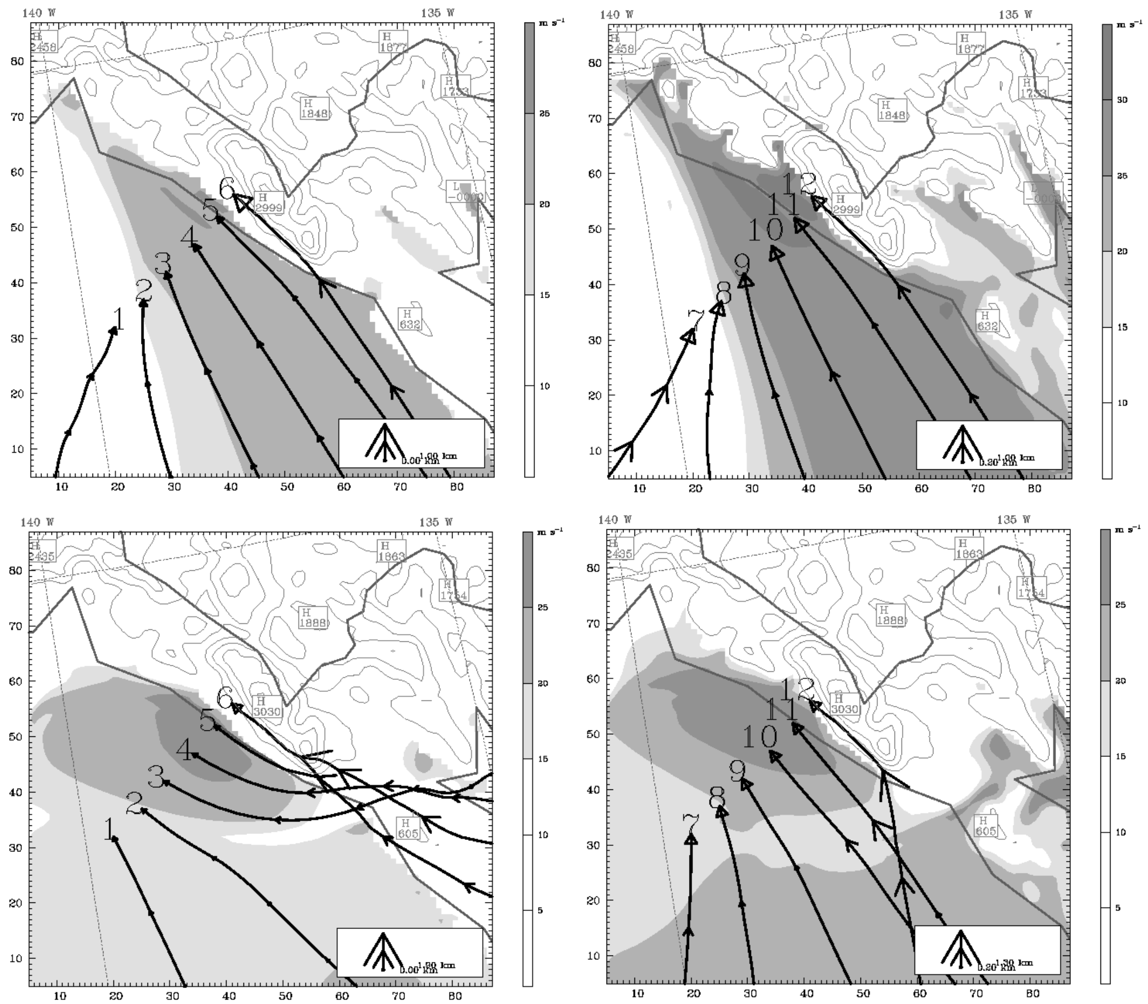

Figure 7. Backwards trajectories for IOP1 released at 2300 UTC September 2004 at (a) 150 m ASL and (b) 500 m ASL and for IOP7 released at 0100 UTC 13 October 2004 at (c) 150 m ASL and (d) 500 m ASL.

runs, respectively, valid for 0000 UTC 13 Oct 2004. The maximum wind speeds exceed 25 m s^{-1} for both simulations; however region of enhanced winds extends about 20-40% further offshore and about 30 km further downstream for CTL than NOGAP. The cross-sections taken through points C-E' (Figs. 8c,d) also show this change in width of the coastal jet, but in addition, reveal a slight thickening of the jet beyond 50 km offshore. Removing the Cross Sound gap effectively alters the structure of the hybrid jet of IOP 7, from a slightly offshore placement of the jet max to one centered over the windward slope/coast, such as that observed in the classical jet of IOP 1. The influence of the dense gap outflow acts to extend the jet more offshore and to thicken the seaward side of the jet.

6. Summary

The Southeastern Alaskan Regional Jets experiment (SARJET) investigated the structure and physical processes of coastal barrier jets along the coastal Fairweather Mountains near Juneau, Alaska. This paper presented in situ aircraft data and high resolution simulations to compare a "classical" barrier jet (IOP 1) with another "hybrid" jet (IOP 7) that had gap flow influences at low-levels.

During IOP 1 there was south-southeasterly flow preceding a landfalling trough, which became blocked by the coastal terrain and accelerated down the pressure gradient to produce a 5-10 m s^{-1} wind enhancement to 30 m s^{-1} in the alongshore direction near the Fairweathers. In contrast, IOP 7 featured higher surface pressure and colder low-level temperatures to the east (inland) of the study area than IOP 1, which resulted in offshore-directed coastal gap flows below ~500 m. The gap flow out Cross Sound gap turned anticyclonically and merged with a southeasterly barrier jet. Unlike the classical jet (IOP1), IOP 7 had a warm anomaly near the coast and a cold anomaly further offshore within the merged gap flow. Above the shallow gap flow at mid-mountain level the flow represented more of a classical barrier jet, with southerly flow deflected and accelerated more parallel to the Fairweathers.

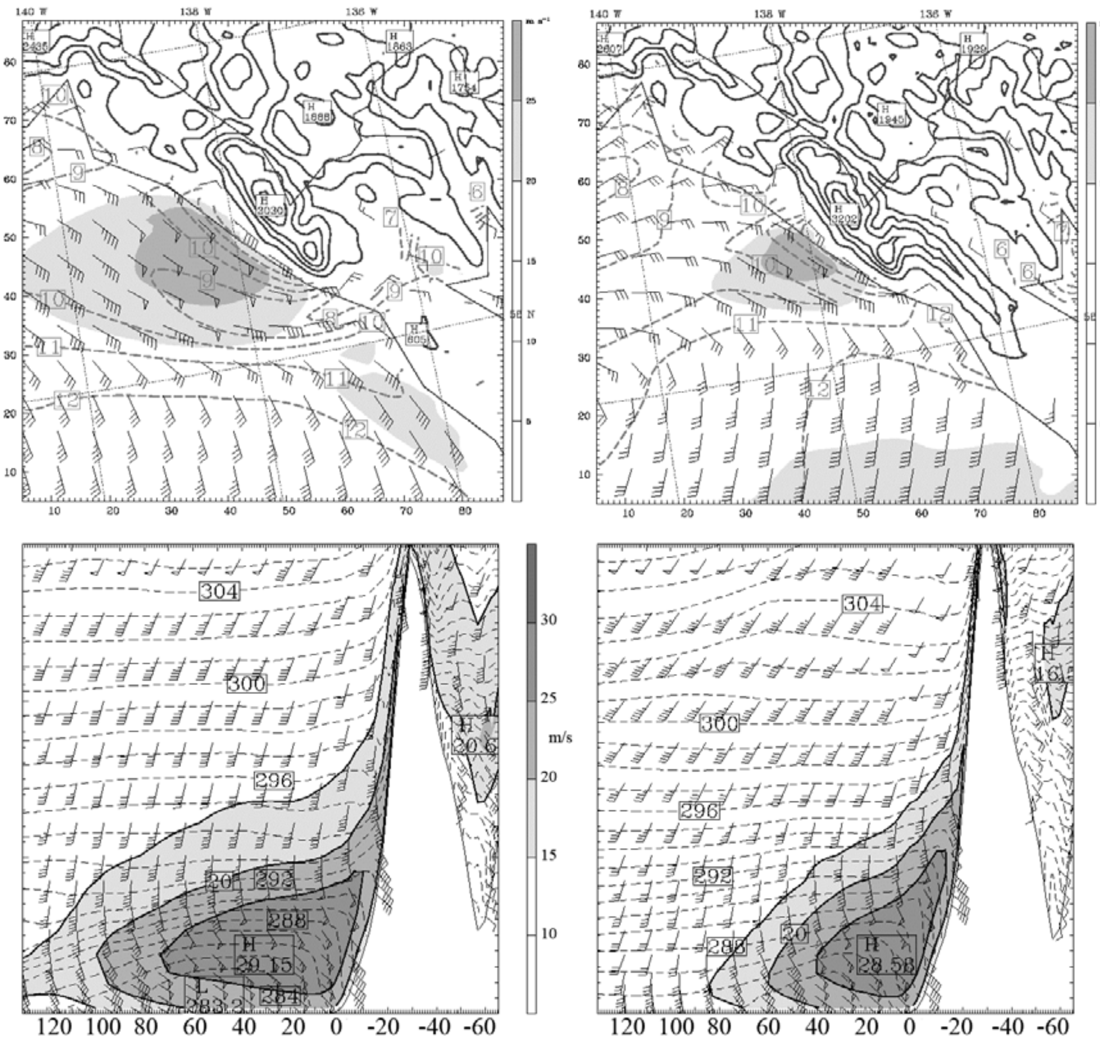

Figure 8. Comparison of CTL and NOGAP experiment showing the winds and temperatures at 150 m ASL for a) CTL and b) DAM and cross-section along C-E' of plane-normal wind speed and potential temperature for c) CTL and d) DAM valid at 2300 UTC 12 October 2004.

Model trajectories show that IOP 1 had only onshore flow origins, while the coastal winds in IOP 7 had both gap and offshore origins near the surface and onshore above mid-mountain level. To test the impact of the gap flow, a simulation was performed with the Cross Sound gap filled. This produced a coastal jet with similar maximum wind speeds, but resulted in a reduction in the width and thickness of coastal jet by about 20-40% and 10-20%, respectively.

Acknowledgements

This research was funded by the National Science Foundation grants ATM-020402 (Colle) and ATM-0240869 (Winstead), and ATM- 0240869 (Bond).

References

Colle, B. A., K. A. Loescher, G. S. Young, and N. S. Winstead, 2006: Climatology of barrier jets along the Alaskan Coast. Part II: Large-scale and sounding composites. *Mon. Wea. Rev.,* **134,** 454-477.

Colle, B. A., and C. F. Mass, 2000: High-resolution observations and numerical simulations of easterly gap flow through the Strait of Juan de Fuca on 9-10 December 1995. *Mon. Wea. Rev.,* **128,** 2398-2422.

Doyle, J. D., 1997: The influence of mesoscale orography on a coastal jet and rainband. *Mon. Wea. Rev.,* **125,** 1465-1488.

Doyle, J. D., and N. A. Bond, 2001: Research aircraft observations and numerical simulations of a warm front approaching Vancouver Island. *Mon. Wea. Rev.,* **129,** 978-998.

Dudhia, J., 1989: Numerical study of convection observed during the winter monsoon experiment using a mesoscale two-dimensional model. *J. Atmos. Sci.,* **46,** 3077-3107.

Grell, G. A., J. Dudhia, and D. R. Stauffer, 1994: A description of the fifth-generation Penn State/NCAR Mesoscale Model (MM5). 122 pp.

Klemp, J. B., and D. R. Durran, 1983: An upper boundary condition permitting internal gravity wave radiation in numerical mesoscale models. *J. Atmos. Sci.,* **111,** 430-444.

Lackmann, G. M., and J. Overland, 1989: Atmospheric structure and momentum balance during a gap-wind event in Shelikof Strait, Alaska. *Mon. Wea. Rev.,* **116,** 1289-1301.

Loescher, K. A., G. S. Young, B. A. Colle, and N. S. Winstead, 2006: Climatology of barrier jets along the Alaskan Coast. Part I: Spatial and temporal distributions. *Mon. Wea. Rev.,* **134,** 437-453.

Macklin, S. A., N. A. Bond, and J. P. Walker, 1990: Structure of a low-level jet over lower Cook Inlet, Alaska. *Mon. Wea. Rev.,* **118,** 2568-2578.

Mass, C. F., S. Bussinger, M. Albright, and Z. A. Tucker, 1995: A windstorm in the lee of a gap in a coastal mountain barrier. *Mon. Wea. Rev.,* **123,** 315-331.

Mass, C. F. and G. K. Ferber, 1990: Surface pressure perturbations produced by an isolated mesoscale topographic barrier. Part I: General charachteristics and dynamics. *Mon. Wea. Rev.,* **118,** 2579-2596.

Mellor, G. L. and T. Yamada, 1974: A hierarchy of turbulence closure models for planetary boundary layers. *J. Atmos. Sci.,* **31,** 1791-1806.

Overland, J. and N. Bond, 1995: Observations and scale ananlysis of coastal jets. *J. Atmos. Sci.,* **42,** 271-282.

Parish, T. R., 1982: Barrier winds along the Sierra Nevada Mountains. *J. Appl. Meteror,* **21,** 925-930.

Seaman, D. R. S. a. N. L., 1994: Multiscale Four-Dimensional Data Assimilation. *J. Appl. Meteor.,* **33,** 416-434.

Winstead, N. S., B. A. Colle, N. A. Bond, G. Young, J. B. Olson, K. Loescher, F. Monaldo, D. Thompson, and W. Pichel, 2006: Barrier jets: combining SAR remote sensing, field observations, and models to better understand coastal flows in the Gulf of Alaska. *Bull. Amer. Meteor. Soc.,* **87,** 787-800.

Zhang, D. and R. Anthes, 1982: A high-resolution model of the planetary boundary layer—sensitivity tests and comparisons with SESAME-79 data. *J. Appl. Meteor.,* **21,** 1594-1609.